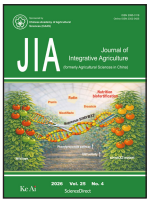
Journal of Integrative Agriculture 2026, 25(4): 1463–1474

Available online at ScienceDirect

Journal of Integrative Agriculture



RESEARCH ARTICLE

CRISPR/Cas9-mediated mutagenesis of transcriptional repressor *SlMYB32* improves flavonols and flavanones accumulation in tomato fruit

Ruining Zhang[1, 2], Yunlin Cao[1, 2], Tong Zhang[1, 2], Yingyue Ma[1, 2], Jiajia Li[1, 2], Kunsong Chen[1, 2], Xian Li[1, 2#]

[1] *College of Agriculture & Biotechnology, Zhejiang University, Hangzhou 310058, China*
[2] *Zhejiang Key Laboratory of Horticultural Crop Quality Improvement, Zhejiang University, Hangzhou 310058, China*

Highlights

- SlMYB32 was identified as a repressor regulating phenylpropanoid pathway.
- CRISPR/Cas9-mediated mutagenesis of *SlMYB32* results in flavonol-rich tomatoes with 1 mg g^{-1} FW rutin.

Abstract

Flavonols and flavanones are important bioactive compounds with multiple pharmacological activities and health benefits. Transcriptional activation of flavonol and flavanone biosynthesis has been studied extensively, while little is known about the negative regulators. CRISPR/Cas9 gene-editing technology, with the advantage of precise genetic modification, is a desirable tool for breeding biofortified materials and exploring potential molecular mechanisms. In this study, a transcriptional repressor, SlMYB32, was characterized in tomato fruit. Phenotype and metabolomic analyses confirmed that knockout of *SlMYB32* resulted in increased accumulation of flavonols and flavanones, especially about 1 mg g^{-1} FW of quercetin 3-*O*-rutinoside (rutin). Transcriptome analysis indicated that expression of key genes *SlPAL6*, *Sl4CL3* and *Sl4CL4* as well as five candidate *SlUGT*s were significantly up-regulated in *slmyb32* mutants. Dual-luciferase and EMSA assays indicated SlMYB32 could bind to and repress promoter activities of *SlPAL6* and *Sl4CL3*. Expression of 27 transcription factors belonging to 12 families was significantly changed in *slmyb32* mutants, among which two SlMYBs, two SlNACs, two SlAP2s and one SlWRKY were clustered with known flavonoid regulators. Our results provide new insights into improving bioactive compounds in fruit and understanding negative regulatory mechanisms in flavonol and flavanone biosynthesis.

Keywords: flavonol, flavanone, CRISPR/Cas9, repressor SlMYB32, tomato, transcriptional regulation

1. Introduction

Flavonols and flavanones are widely distributed in plants and play significant roles in regulating plant growth and development, and improving stress resistance (Tohge and Fernie 2016; Murata *et al.* 2020; Saxena *et al.* 2023). Derivatives of quercetin and kaempferol are major flavonol compounds, and naringenin derivatives are important flavanones in plants. Quercetin and its glycosides, such as quercetin 3-*O*-rutinoside (Q3Rut, rutin) are superior therapeutic components in cancer and diabetes (Pathak *et al.* 2018; Tang *et al.* 2023). Kaempferol and its derivatives possess strong anti-bacterial and neuroprotective activity (Lin *et al.* 2020; Han *et al.* 2021). Naringenin and its derivatives with antioxidant activity exhibit important anti-cancer potentials (Kumar *et al.* 2015). Thus, enhancement of flavonol or flavanone levels contributes to nutrient-biofortification in plant-based foods.

Biosynthesis of flavonols and flavanones is well understood and consists of phenylpropanoid and flavonoid pathways (Fig. 1). Phenylalanine ammonia lyase (PAL), cinnamate 4-hydroxylase (C4H), and 4-coumaroyl CoA ligase (4CL) constitute the phenylpropanoid pathway, which contributes to the production of *p*-coumaroyl CoA from phenylalanine. *p*-Coumaroyl CoA is catalyzed to form naringenin under the

Received 31 January 2025; Received in revised form 8 June 2025; Accepted 25 September 2025; Available online 13 November 2025
Ruining Zhang, E-mail: rnzh@zju.edu.cn; #Correspondence Xian Li, E-mail: xianli@zju.edu.cn

© 2026 CAAS. Publishing services by Elsevier B.V. on behalf of KeAi Communications Co. Ltd. This is an open access article under the CC BY-NC-ND license (http://creativecommons.org/licenses/by-nc-nd/4.0/). Peer review under responsibility of Editorial Board of *Journal of Integrative Agriculture*.
doi: 10.1016/j.jia.2025.11.011

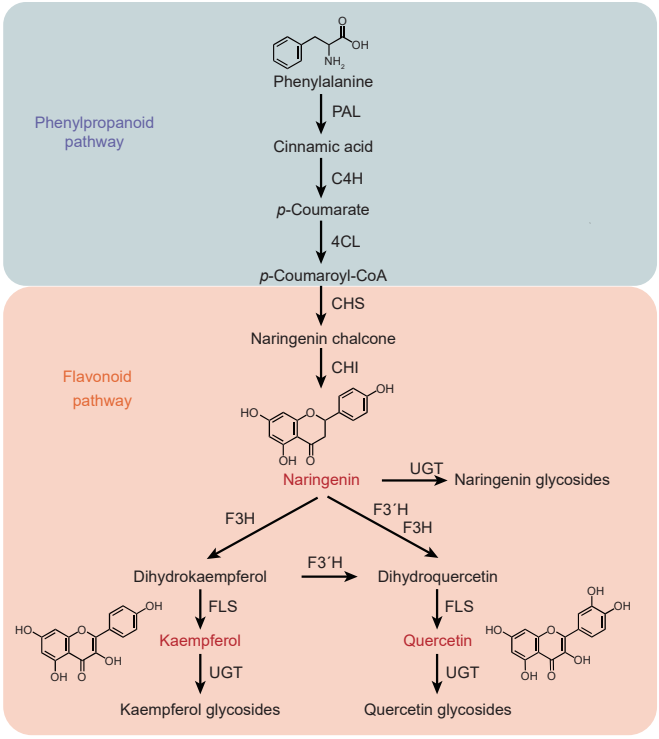


Fig. 1 Biosynthesis of flavonols and flavanones consisting of phenylpropanoid and flavonoid pathways. Phenylalanine ammonia lyase (PAL), cinnamate 4-hydroxylase (C4H), and 4-coumaroyl CoA ligase (4CL) constitute the phenylpropanoid pathway. *p*-Coumaroyl CoA is catalyzed to form naringenin under the action of chalcone synthase (CHS) and chalcone isomerase (CHI). Kaempferol and quercetin are produced from naringenin through enzymatic reactions including flavanone 3-hydroxylase (F3H), flavonoid 3′-hydroxylase (F3′H), and flavonol synthase (FLS). Flavanone and flavonol glycosides are formed by UDP-glycosyltransferases (UGTs).

action of chalcone synthase (CHS) and chalcone isomerase (CHI). Kaempferol and quercetin are produced from naringenin through multiple enzymatic reactions including flavanone 3-hydroxylase (F3H), flavonoid 3′-hydroxylase (F3′H), and flavonol synthase (FLS). Flavanone and flavonol glycosides are formed from naringenin, kaempferol and quercetin with different glycosylations by UDP-glycosyltransferases (UGTs).

Based on the pathway, increasing transcriptional regulatory mechanisms have been uncovered. The MYB family, especially R2R3-MYB, is recognized as central regulator involved in flavonol biosynthesis (Cao *et al.* 2024a), and MYB activators have been studied widely in fruit (Czemmel *et al.* 2009; Li H *et al.* 2020; Xing *et al.* 2021a). Also, negative regulators are important factors regulating metabolic homeostasis. Increasing studies have reported transcription repressors are involved in anthocyanin biosynthesis. Arabidopsis AtMYB4 was found to repress activity of *AtC4H* promoter (Jin *et al.* 2000). PhMYB27 and VvMYBC2-L1 was reported to inhibit anthocyanin accumulation in *Petunia hybrida* and *Vitis vinifera*, respectively (Albert *et al.* 2014; Cavallini *et al.* 2015). However, transcription repressors involved in flavonol or flavanone biosynthesis are lack of in-depth studies.

CRISPR/Cas9 gene-editing technology has received widespread attention due to its superiority of precise gene modifications (Rodríguez-Leal *et al.* 2017; Zhang and Zhu 2024). Deletion of autoinhibitory domain of key biosynthetic enzymes SlGAD2 and SlGAD3 using CRISPR/Cas9 resulted in high γ-aminobutyric acid (GABA) accumulation in tomato fruit (Nonaka *et al.* 2017). Knockout of biosynthetic gene *Sl7-DR2* hindered conversion of provitamin D3 and improved UVB-induced accumulation of vitamin D3 in fruit (Li J *et al.* 2022). Thus, CRISPR/Cas9 targeting structural genes is an important strategy for nutrition improvement. However, CRISPR/Cas9-targeted mutagenesis of transcriptional repressors would be another strategy to improve nutrients, which need further investigation.

Tomato is a model fruit for nutrient improvement and mechanism exploration because of its high-quality genomes and stable genetic transformation (Shi *et al.* 2024). In this study, one negative regulator SlMYB32 was characterized to be involved in flavonol and flavanone biosynthesis, and tomato enriched with rutin of 1 mg g^{-1} fresh weight (FW) was obtained by CRISPR/Cas9-induced mutagenesis of *SlMYB32*. Metabolome, transcriptome and transcriptional regulation analyses were conducted in *slmyb32* mutants and wild type (WT), to reveal the potential regulatory mechanisms underlying flavonol and flavanone pathway. The results provide a useful route to nutrient improvement in plant-based food and deepen our understanding of the negative regulatory mechanisms in flavonol and flavanone biosynthesis.

2. Materials and methods

2.1. Sequence alignment and phylogenetic analysis

Full-length amino acid sequences of SlMYB3, SlMYB7 and SlMYB32 were obtained from the Phytozome database (https://phytozome-next.jgi.doe.gov/). Amino acid sequence alignments were performed by DNAMAN and ClustalX 1.81 softwares. The phylogenetic tree was constructed *via* the neighbor-joining method using MEGA V7.0 software with the bootstrap values from 1,000 replicates (Xing *et al.* 2021b).

2.2. Quantitative real-time PCR

Total RNA of tomato fruit peel samples was extracted using the CTAB method (Xing *et al.* 2021b). cDNA was synthesized using PrimeScript RT Reagent Kit with gDNA Eraser (TaKaRa, Beijing, China). Quantitative real-time PCR (RT-qPCR) was performed using a Bio-Rad CFX96 instrument (Bio-Rad, California, USA). Expression of genes was analyzed using $2^{-\Delta Ct}$ and *SlACTIN* was used as reference gene (Liu *et al.* 2020). All primers used for RT-qPCR are listed in Appendix A.

2.3. Flavonol and flavanone analysis

Flavonol and flavanone compounds were identified by their retention times and absorbances at 370 nm according to Cao *et al.* (2024b) with some modifications. Peel of tomato fruit at break+7 stage was sampled with three biological replicates, and eight fruit was pooled for each replicate. Sample powder (0.1 g) was extracted in 1 mL of 50% methanol with sonication for 30 min at room temperature. After three cycles of centrifugation at 12,000 r min^{-1} for 15 min, the supernatant was filtered by 0.22 μm

filter and applied to high performance liquid chromatography (HPLC) photodiode-array detection (DAD) system (e2695 pump, 2998 PDA detector; Waters, Massachusetts, USA) and Sunfire C18 ODS column (4.6 mm×250 mm; Waters, Massachusetts, USA). The mobile phase was 0.1% formic acid in water (eluent A) and 0.1% formic acid in 50% acetonitrile aqueous solution (eluent B). The gradient program was used as follows: 0 min, 23% eluent B; 45 min, 50% eluent B; 50 min, 100% eluent B; 55 min, 100% eluent B; 56 min, 23% eluent B; 60 min, 23% eluent B. Q3Rut, kaempferol 3-*O*-rutinoside (K3Rut) and naringenin 7-*O*-glucoside (N7Glc) contents were calculated by comparing with their corresponding standard curves, and were represented as μg g^{-1} FW.

2.4. Subcellular localization

Full-length coding sequence of *SlMYB32* was inserted into pCambia2300-eGFP vector to produce *SlMYB32*-eGFP. Recombinant vector and control vector were transformed into *Agrobacterium tumefaciens* GV3101 for transient expression in *Nicotiana benthamiana* leaves (Zhang *et al*. 2022). Tobacco leaves were examined by confocal laser scanning microscope (LSM 880, Carl zeiss, Oberkochen, Germany) after 48 h of culture in the greenhouse. Nucleus-RFP was served as a nuclear marker. Primers used for vector construction are shown in Appendix B.

2.5. Vector construction and tomato transformation

CRISPR/Cas9 gene-editing was performed according to Gao *et al.* (2022) with minor modifications. An online tool CRISPR-P (http://crispr.hzau.edu.cn/cgi-bin/CRISPR2/CRISPR) was used to generate and select target sequences for *SlMYB32* (Appendix C). Two single-guide RNAs (sgRNAs) were cloned into the pYLCRISPR/Cas9 vector using the Golden Gate ligation method (Ma *et al.* 2015). Primers used for recombinant vector construction are shown in Appendix D. The pYLCRISPR/Cas9-*SlMYB32* vector was transformed into *A. tumefaciens* EHA105 for stable transformation of Micro-Tom tomato. The *SlMYB32* knockouts were selected for mutation analysis by PCR using primers flanking the target sites and putative off-target sites (Appendix E). The *slmyb32* homozygous mutants were used for planting and fruit sampling in this study.

2.6. Metabolite identification and data analysis

Widely targeted metabolome analysis of fruit peel for *slmyb32*-#2 mutant and WT was performed by Metware Biotech Co., Ltd. (Wuhan, China) with ultra performance liquid chromatography tandem mass spectrometry (UPLC-MS/MS). Differentially accumulated metabolites (DAMs) were defined as metabolites with 'fold change≥2 or ≤0.5' and 'VIP≥1'. Identified DAMs were classified and enriched into the Kyoto Encyclopedia of Genes and Genomes (KEGG) pathway. Significant enrichment pathway of DAMs indicated enrichment with $P<0.05$. Metabolome data statistics were completed on the Metware cloud platform (Wuhan, China).

2.7. Transcriptome sequencing and data analysis

Total RNA was extracted from peel samples of *slmyb32*-#2 mutant and WT at break+7 stage with the CTAB method (Xing *et al.* 2021b) to check the purity and integrity. RNA library construction and sequencing were performed by Novogene Tech Co., Ltd. (Beijing, China). RNA-seq data were generated from the library using the Illumina platform. After raw read filtering and correction, clean reads were mapped to the reference genome *Solanum lycopersicum* ITAG4.0 (https://www.solgenomics.net/organism/Solanum_lycopersicum/genome). Read counts were calculated with featureCounts, and fragments per kilobase of exon model per million mapped fragments (FPKM) values were calculated for gene expression. Differentially expressed genes (DEGs) were identified using DESeq2 (Love *et al.* 2014) based on 'fold change≥2 or ≤0.5' and '$P<0.05$'. Functional annotation of DEGs was performed by Gene Ontology (GO) enrichment and KEGG enrichment analyses.

2.8. Dual-luciferase assay

Transactivation activities of transcription factors (TFs) on target promoters were detected with dual-luciferase assays according to Cao *et al.* (2023). The full-length coding sequence of *SlMYB32* was cloned into pGreen II 0029 62-SK vectors with primers. The promoters of *SlPAL6*, *Sl4CL3* and *Sl4CL4* were cloned into pGreen II 0800-LUC vectors with primers. Primers are listed in Appendix B, and all constructs were electroporated into *A. tumefaciens* GV3101. The bacteria were prepared in infiltration buffer (10 mmol L^{-1} MES, 10 mmol L^{-1} $MgCl_2$, 150 mmol L^{-1} acetosyringone, pH 5.6) and used when the optical density at 600 nm reached 0.75. *Agrobacterium tumefaciens* mixtures containing SlMYB32 (1 mL) and promoters (100 μL) were infiltrated into 4-week-old *N. benthamiana* leaves. The firefly luciferase (LUC) and renilla luciferase (REN) was detected using Dual-Luciferase Reporter System (Promega, Madison, USA) after 3 d infiltration. The ratios of LUC and REN were expressed as transactivation activities. Six biological replicates were used for each measurement in all experiments.

2.9. Protein purification and electrophoretic mobility shift assay (EMSA)

Protein purification was conducted according to Ren *et al.* (2022). Coding sequence of *SlMYB32* was cloned into the pET32a vector, and construct was transformed into *Escherichia coli* Transetta (DE3) (TransGen Biotech, Beijing, China). Protein were induced by 0.5 mmol L^{-1} isopropyl-β-D-thiogalactopyranoside (IPTG) and purified with ProteinIso Ni-NTA-Resin affinity chromatography columns (TransGen Biotech, Beijing, China). EMSA were carried out according to chemiluminescence kit instructions (Thermo Fisher, Waltham, USA). Probes were biotin-labelled at the 3′ end of primers, while cold probes were unlabeled. Primer and probe sequences were provided in Appendix B.

2.10. Statistical analysis

All data were obtained with at least three biological replicates, and error bars indicate standard errors. Statistical significance was analyzed by a two-tailed Student's *t*-test using SPSS 19.0 software (IBM Corp., Armonk, USA). All figures were produced by GraphPad Prism 8 or TBtools-II v2.119 (Chen *et al.* 2023).

3. Results

3.1. Isolation and characterization of MYB repressors in tomato

Phylogenetic analysis was performed between MYB proteins from tomato, Arabidopsis, and apple, etc. MYB phylogenetic tree was divided into five clades based on functions of MYB proteins, including flavonol, anthocyanin, and proanthocyanidin, R3 repressor and R2R3 repressor (Fig. 2-A). It was demonstrated that SlMYB3, SlMYB7 and SlMYB32 were clustered with known repressors AtMYB4, AtMYB7 and MdMYB16 (Fig. 2-A). Sequence analysis revealed *SlMYB3*, *SlMYB7* and *SlMYB32* encode 837, 756, and 822 bp coding sequence, respectively, indicating that SlMYB3, SlMYB7 and SlMYB32 encoded predicted proteins containing 279, 252 and 274 amino acid residues, respectively. Amino acid sequence analysis showed that SlMYB3, SlMYB7 and SlMYB32 all possessed two adjacent MYB repeats in their conserved DNA-binding domain, and one conserved C1 motif and one predicted ethylene-responsive element binding factor-associated amphiphilic repression (EAR) domain with repressive function were found in three proteins (Fig. 2-B). The above results suggest that SlMYB3, SlMYB7 and SlMYB32 are candidate R2R3 repressors involved in flavonoid biosynthesis.

3.2. Correlation between flavonol content and gene expression of MYB candidates

It was revealed that flavonol accumulated gradually with fruit development, reaching a maximum at Break+7 stage (Fig. 3-A). Expression of *SlMYB32* reached a high level in fruits at mature green (MG) stage, and then its expression level gradually decreased as fruit matured (Fig. 3-B). Relative expression of both *SlMYB3* and *SlMYB7* was maintained at a low level from MG to Break+7 stage (Fig. 3-B). Expression of *SlMYB32* was negatively correlated with flavonol content during fruit development, indicating that SlMYB32 could be a potential candidate to negatively regulate flavonol biosynthesis in tomato. Subcellular localization analysis showed that green fluorescence of *SlMYB32*-eGFP merged with red fluorescence signal in nucleus, manifesting that *SlMYB32* localizes to the nucleus (Fig. 3-C). These results indicate that SlMYB32 is a nuclear-localized candidate repressor involved in flavonol accumulation.

3.3. CRISPR/Cas9-mediated knockout of *SlMYB32* in tomato

The two targeted sites were located on the second exon of *SlMYB32* (Fig. 4-A), and two *slmyb32* homozygous mutants, *slmyb32*-#1 and *slmyb32*-#2, were obtained using CRISPR/Cas9 gene-editing system to confirm the function (Fig. 4-B). A 17 bp deletion was found at the second target site of *slmyb32*-#1 mutant. In *slmyb32*-#2 mutant, 4 bp deletion at the first target site and 7 bp deletion at the second target site were detected. There were 115 and 102 amino acid residues of SlMYB32 detected in *slmyb32*-#1 and *slmyb32*-#2 mutants, respectively (Fig. 4-C). Neither mutant contained the C1 motif and EAR domain, indicating two *slmyb32* mutants might lose their repressive function (Fig. 4-C).

Fruit phenotypes showed fruit color of both *slmyb32* mutants at Break+7 stage changed from red to orange (Fig. 4-D). HPLC analysis showed Q3Rut and K3Rut contents in fruit of *slmyb32*-#1 mutant were twice that of the WT (Fig. 4-E). Likewise, Q3Rut content reached nearly 1 mg g^{-1} FW and K3Rut content was increased to three times in fruit of *slmyb32*-#2 mutant that of the WT (Fig. 4-E). In addition to flavonol levels, a significant 2–4 folds increase in N7Glc content was observed in two *slmyb32* mutants (Fig. 4-E). These findings indicate that knockout of repressive functional motifs in *SlMYB32* significantly improves both flavonols and flavanones accumulation in fruit.

3.4. Metabolome analysis for fruit of *slmyb32* mutants

A total of 814 metabolites were detected and quantified, encompassing 12 metabolite classes (Appendix F), of which flavonoids are major components of the DAMs (Appendix G). KEGG enrichment analysis of DAMs showed that significantly enriched pathways included flavonoid biosynthesis, caffeine metabolism and terpenoid backbone biosynthesis (Fig. 5-A). Heatmap diagram indicated that differentially accumulated flavonols and flavanones were up-regulated in *slmyb32*-#2 mutant (Fig. 5-B). Up-regulated flavonols included four quercetin derivatives, three kaempferol derivatives and three isorhamnetin derivatives (Fig. 5-B). Naringenin glycosides were main differentially accumulated flavanones, such as naringenin 7-*O*-glucoside, naringenin 7-*O*-neohesperidoside, and naringenin 7-*O*-rutinoside (Fig. 5-B). Hesperetin derivatives and persicoside were also differentially accumulated in the mutant (Fig. 5-B). These results suggest that knockout of *SlMYB32* significantly influences flavonoid biosynthesis, especially increases flavonol and flavanone accumulation.

3.5. Transcriptome analysis for fruit of *slmyb32* mutants

DEGs were analyzed between *slmyb32*-#2 mutant and WT using RNA-Seq to investigate regulatory mechanisms of SlMYB32. There were 492 DEGs detected in *slmyb32*-#2 mutant fruit compared with WT (Appendix H). It was shown that the DEGs were annotated to 422 GO terms, and significantly enriched to 58 GO terms (Appendix I). The top 10 enriched GO terms for category of biological process (BP), cellular component (CC) and molecular function (MF) were shown in Fig. 6-A. The main terms of BP category included response to biotic stimulus (GO: 0009607), aminoglycan metabolic process (GO: 006022) and aminoglycan catabolic process (GO: 0006026). The most enriched term in CC category was apoplast (GO: 0048046). The main GO terms of MF category were ion channel activity (GO: 0005216), channel activity (GO: 0015267) and passive transmembrane transporter activity (GO: 0022803).

KEGG enrichment analysis showed that 492 DEGs were assigned to 73 KEGG pathways, of which nine pathways were significantly enriched (Appendix J). The most significant enriched KEGG pathway was phenylpropanoid biosynthesis (Fig. 6-B). KEGG pathways of phenylalanine metabolism as well as flavonoid biosynthesis were also

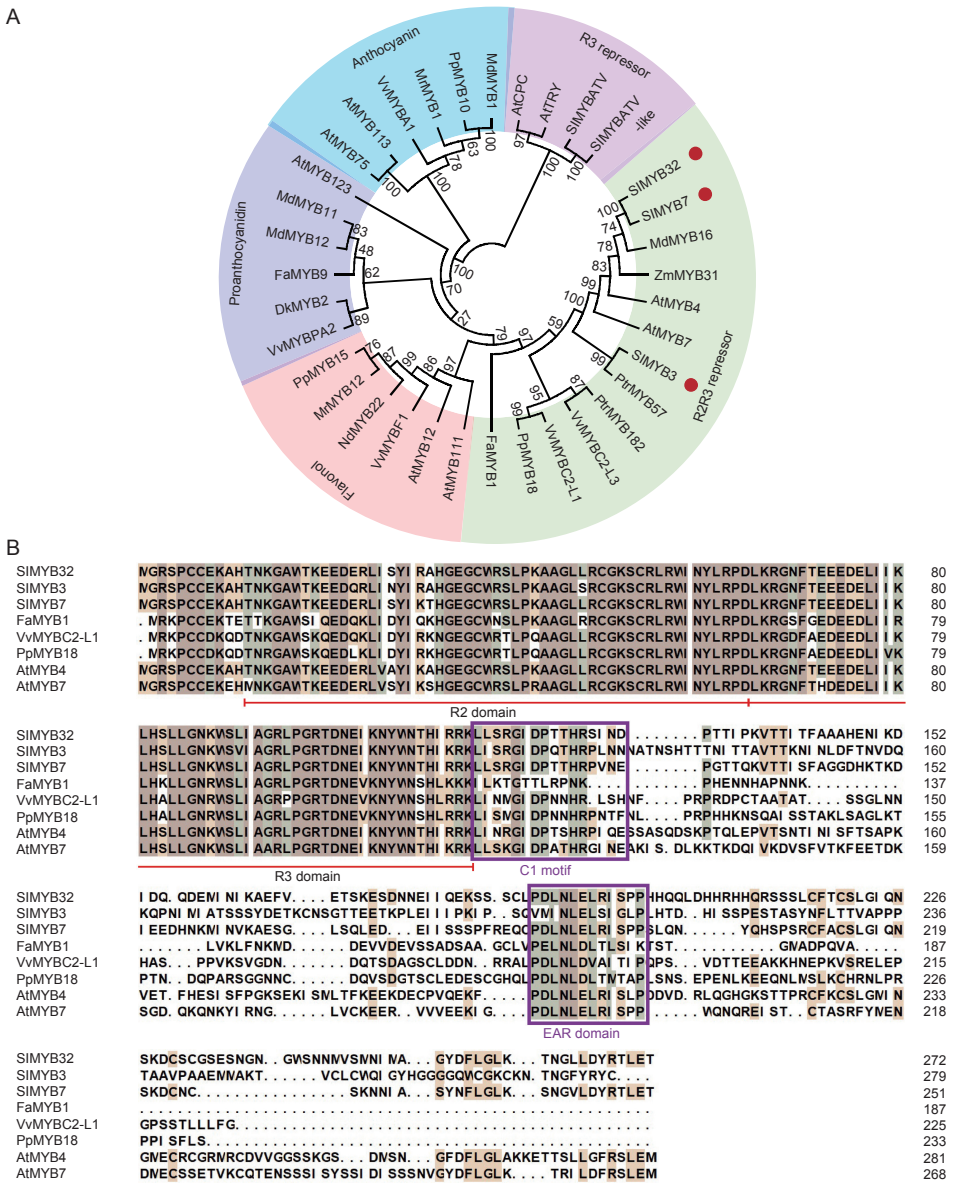


Fig. 2 Phylogenetic analysis and sequence alignment of SlMYB3, SlMYB7 and SlMYB32. A, phylogenetic analysis of MYB proteins involved in flavonoids biosynthesis in tomato and other species. Three R2R3-MYB repressors are highlighted with the solid green circle. B, amino acid sequence alignment of SlMYB3, SlMYB7, SlMYB32 and other known flavonoid-related R2R3-MYB repressors in plants. Conserved residues are marked in brown and partial conservation is shown in orange. The R2 and R3 domains are indicated with red lines, whereas C1 motif and EAR domain in the C-terminus are boxed and numbered. Accession number is listed as follows: *Arabidopsis thaliana* AtMYB4 (NP_195574), AtMYB7 (NP_179263), AtMYB12 (NP_182268), AtMYB75 (NP_176057), AtMYB111 (NP_199744), AtMYB113 (NP_176811), AtMYB123 (NP_198405), AtCPC (NP_182164), AtTRY (NP_200132); *Malus domestica* MdMYB1 (ADB25061), MdMYB11 (AAZ20431), MdMYB12 (ADL36755), MdMYB16 (ADL36756), MdMYB22 (AAZ20438); *Vitis vinifera* VvMYBA1 (BAD18977), VvMYBPA2 (ACK56131), VvMYBF1 (ACV81697), VvMYBC2-L1 (AFX64995), VvMYBC2-L3 (AIP98385); *Prunus persica* PpMYB10 (ADK73605), PpMYB15 (ONH94094), PpMYB18 (ALO81021); *Solanum lycopersicum* SlMYBATV (NP_001352307), SlMYBATV-like (TMW99237), SlMYB3 (XP_004241841), SlMYB7 (XP_004231034), SlMYB32 (NP_001233975); *Morella rubra* MrMYB1 (ADG21957), MrMYB12 (KAB1200696); *Fagaria* × *ananassa* FaMYB1 (AAK84064), FaMYB9 (AFL02460); *Populus tomentosa* PtrMYB57 (XP_002325733); *Populus tremula*×*Populus tremuloides* PtMYB182 (AJI76863); *Diospyros kaki* DkMYB2 (BAI49719); *Zea mays* ZmMYB31 (NP_001105949).

significantly enriched with the DEGs. The above results suggest that mutations in *SlMYB32* significantly affected phenylpropanoid and flavonoid metabolic pathways.

3.6. Repressive effect of SlMYB32 on phenylpropanoid pathway

Expression analysis of flavonol and flavanone biosynthetic genes showed that structural genes *SlPAL6*, *Sl4CL3* and *Sl4CL4* were significantly up-regulated in *slmyb32*-#2 mutant (Fig. 7-A). Expression of other genes including *SlPAL1*, *SlPAL3*, *SlPAL4*, *SlPAL5*, *Sl4CL1*, *Sl4CL2*, *Sl4CL5*, *Sl4CL6*, *SlCHS1*, *SlCHS2*, *SlCHI*, *SlF3H*, *SlF3′H* and *SlFLS* in flavonoid pathway manifested no significant difference (Appendix K). These results indicate that SlMYB32 may

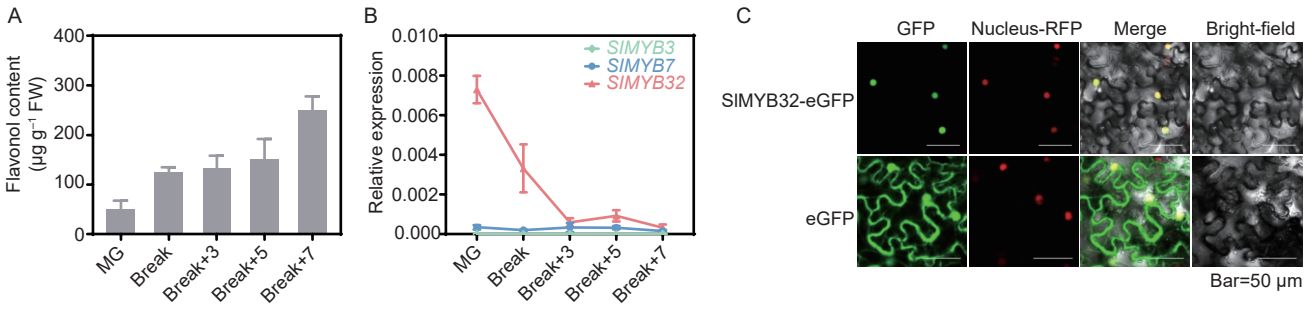


Fig. 3 Flavonol content, gene expression, and subcellular localization of candidate MYB repressors. A, flavonol content in wild type tomato fruit during developmental stages by high performance liquid chromatography (HPLC). B, relative expression level of *SlMYB3*, *SlMYB7* and *SlMYB32* in wild type tomato fruit at mature green (MG), break, break+3, break+5 and break+7 stages. C, subcellular localization of SlMYB32 in *Nicotiana benthamiana* leaf cells.

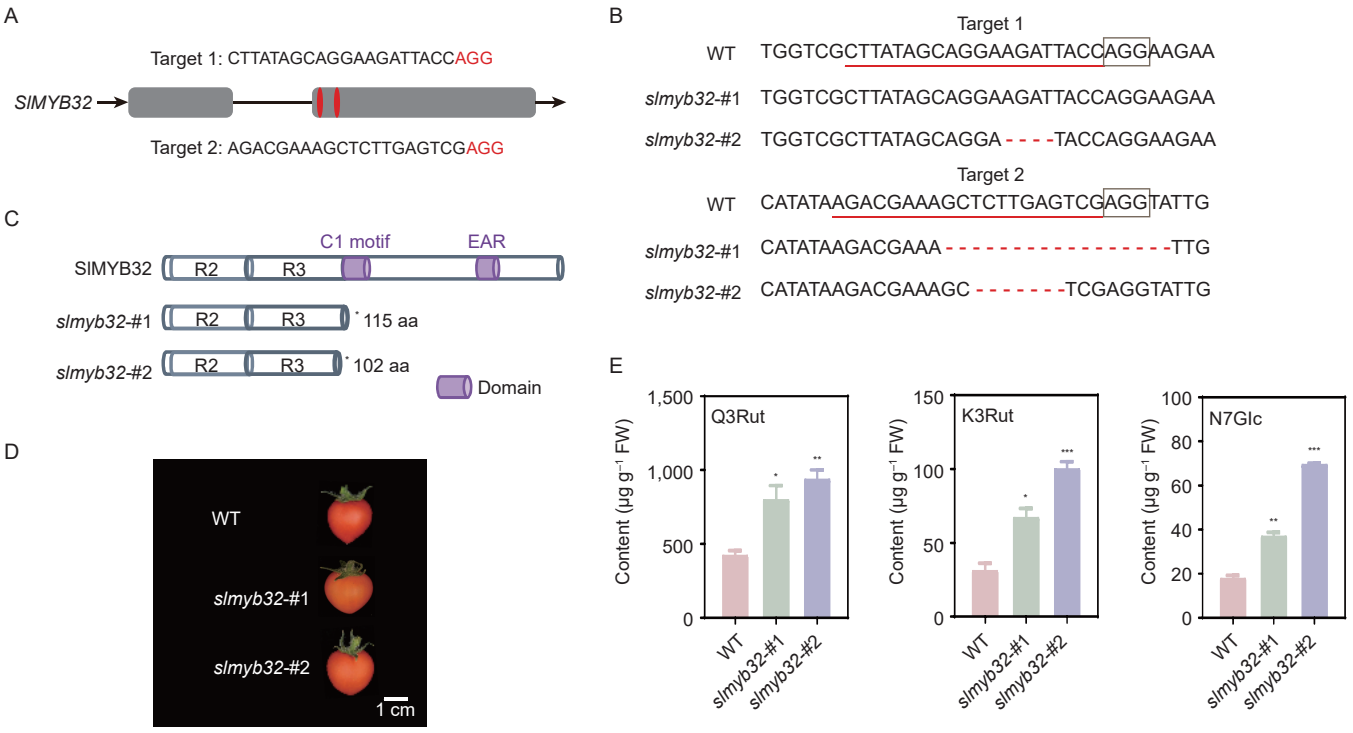


Fig. 4 CRISPR/Cas9-induced mutations in the *SlMYB32* gene. A, a schematic map of the sgRNA targeted sites on the genomic regions of *SlMYB32*. The intergenic region and introns are shown as lines; the exons are shown as gray boxes. The protospacer adjacent motifs (PAMs) are shown in red. B, sequencing results of the *slmyb32* homozygous mutant lines. The PAM is boxed, the target sequence is underlined, and the dashes indicate deletions. C, protein structure diagram of the *slmyb32* homozygous mutant lines. The purple columns indicate domains. D, the phenotype of the fruit of wild type (WT) and *slmyb32* homozygous mutants (*slmyb32*-#1 and *slmyb32*-#2) at break+7 stage. E, quercetin 3-*O*-rutinoside (Q3Rut), kaempferol 3-*O*-rutinoside (K3Rut) and naringenin 7-*O*-glucoside (N7Glc) content of the fruit of WT as well as *slmyb32*-#1 and *slmyb32*-#2 mutants at break+7 stage. Data were means of three biological replicates and error bars indicated standard errors. Statistical significance was determined by Student's *t*-test (*, $P<0.05$; **, $P<0.01$; ***, $P<0.001$).

regulate expression of *SlPAL6*, *Sl4CL3* and *Sl4CL4* involved in the phenylpropanoid pathway.

Dual-luciferase assays showed that SlMYB32 significantly repressed the promoter activity of *SlPAL6* and *Sl4CL3* (both 0.5-fold lower than that of empty vector) (Fig. 7-B). SlMYB32 showed no direct transcriptional repression effect on *Sl4CL4* promoter (Fig. 7-B). EMSA assay was performed to confirm the protein-DNA interaction of SlMYB32 with promoters of *SlPAL6* and *Sl4CL3*. It was shown that SlMYB32 was able to bind to 'TAACCG' of *SlPAL6* promoter and 'ACCAA' of *S4CL3* promoter (Fig. 7-C and D). The results indicate that SlMYB32 may bind to *SlPAL6* and *Sl4CL3* promoters to transcriptionally repress their activities.

3.7. Regulation of SlMYB32 on candidate *SlUGT*s

Among 175 *SlUGT*s, nine *SlUGT*s were significantly up-regulated in *slmyb32* mutant (Fig. 8). Among these nine *SlUGT*s, we focused on 3-*O*-glucosyltransferase (3-*O*-GlcT) and 1,6-rhamnosytransferase (1,6-

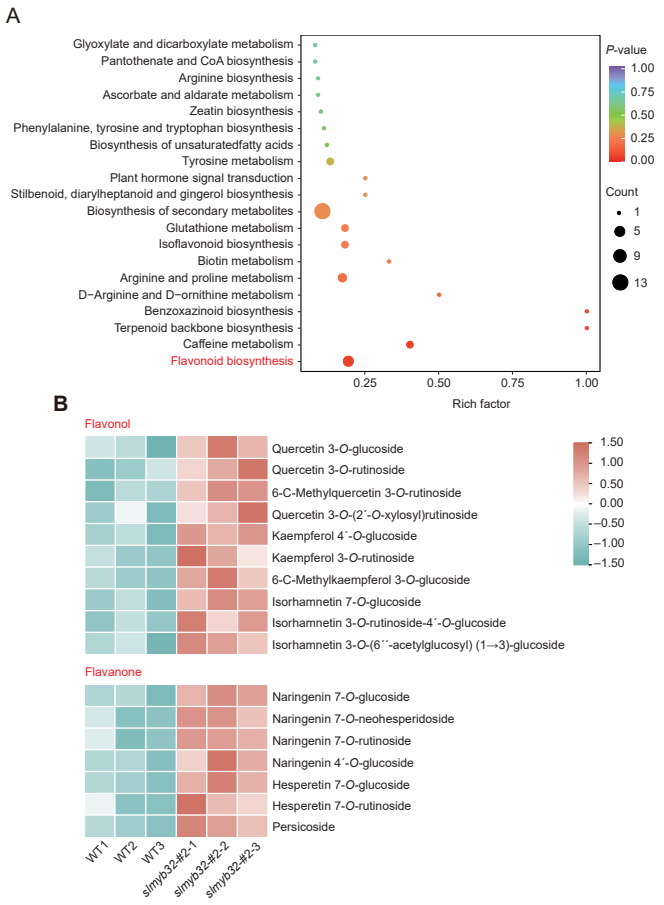


Fig. 5 Differentially accumulated metabolites (DAMs) analysis in *slmyb32*-#2 mutant. A, Kyoto Encyclopedia of Genes and Genomes (KEGG) enrichment analysis for DAMs between WT and *slmyb32*-#2. B, heatmap illustration of $\log_2$-transformed normalized values of flavonols and flavanones between WT and *slmyb32*-#2.

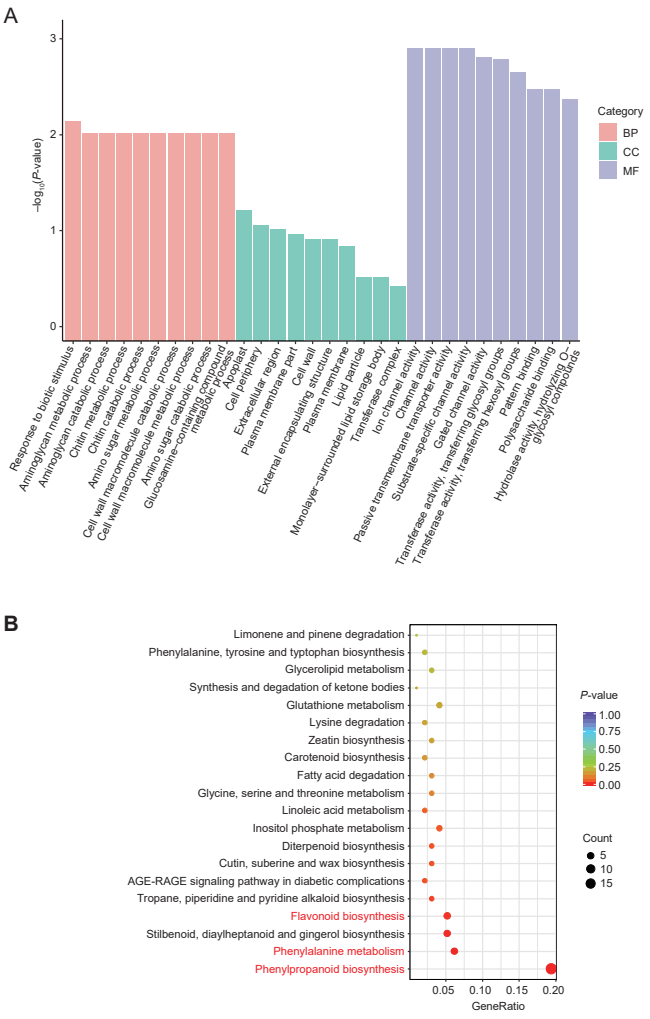


Fig. 6 Enrichment analysis of differentially expressed genes (DEGs) in *slmyb32*-#2 mutant. A, top 10 Gene Ontology (GO) enrichment terms of DEGs between WT and *slmyb32*-#2. BP, biological process; CC, cellular component; MF, molecular function. B, Kyoto Encyclopedia of Genes and Genomes (KEGG) enrichment analysis for DEGs between WT and *slmyb32*-#2.

RhaT) that are necessary for formation of Q3Rut and K3Rut, and 7-*O*-glucosyltransferase (7-*O*-GlcT) that is important for N7Glc formation (Fig. 4-E). As a result, five SlUGTs, i.e., SlUGT85A2 (Solyc12g057060) and SlUGT85A4 (Solyc03g083650) clustered with known 3-*O*-GlcTs, SlUGT73D1 (Solyc10g085860), SlUGT73C3 (Solyc10g083860) and SlUGT72E1 (Solyc02g085660) clustered with known 7-*O*-GlcTs, were identified (Fig. 8-A). Gene expression showed that these five candidate *SlUGT*s *SlUGT85A2*, *SlUGT85A4*, *SlUGT73D1*, *SlUGT73C3*, and *SlUGT72E1* were significantly up-regulated in *slmyb32*-#2 mutant (Fig. 8-B), indicating that SlMYB32 might regulate SlUGT activity to modulate flavonol and flavanone accumulation.

3.8. Analysis of transcription factors involved in flavonol and flavanone biosynthesis

There were 27 differentially expressed TFs (DETFs) of 12 families detected between *slmyb32*-#2 mutant and WT, including AP2, B3, bZIP, bHLH, HSF, MYB, NAC, HD-ZIP, WRKY, C2H2, BBX and Dof (Fig. 9-A). Most of the DETFs, were up-regulated in *slmyb32* mutants compared with WT. Among these DETFs, the top three in number were AP2, NAC and MYB (Fig. 9-A). Of five AP2 DETFs, *Solyc04g012050*, *Solyc12g056980*, *Solyc06g068830* and *Solyc03g120840* were up-regulated, and *Solyc03g093550* was down-regulated in *slmyb32*-#2 mutant. Four DETFs belonging to NAC family were detected, of which *Solyc02g088180*, *Solyc04g005610* as well as *Solyc06g069710* were up-regulated, and *Solyc01g021730* was down-regulated in *slmyb32*-#2 mutant. *Solyc02g090400* and *Solyc05g053330* belonging to MYB family were up-regulated and one MYB DETF *Solyc02g087960* was down-regulated in *slmyb32*-#2 mutant. Two DEGs encoding WRKY, *Solyc05g015850* and *Solyc08g081610* were up-regulated in *slmyb32*-#2 mutant.

Phylogenetic analysis of DETFs and known transcription regulators was conducted, to analyze the relationship between key DETFs and flavonol or flavanone accumulation (Fig. 9-B). Solyc02g087960 and Solyc05g053330 showed strong clustering relations with anthocyanin regulators

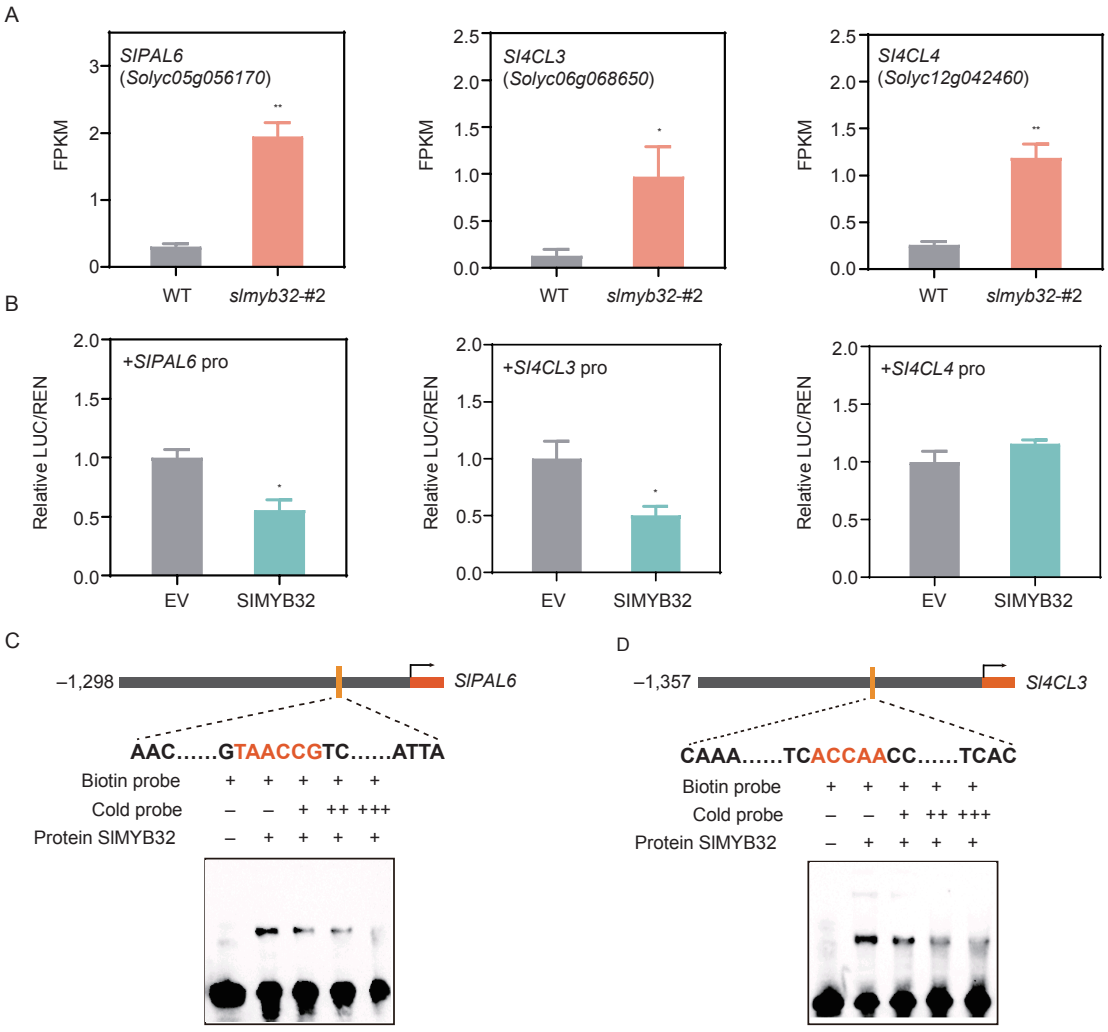


Fig. 7 Regulatory effect analysis of key genes involved in flavonol and flavanone biosynthesis. A, expression analysis of phenylpropanoid pathway genes. B, transcriptional regulatory effect of SlMYB32 to promoters of *SlPAL6*, *Sl4CL3* and *Sl4CL4*. Error bars indicate the standard error of six biological replicates. C, EMSA of SlMYB32 to *SlPAL6* promoter. D, EMSA of SlMYB32 to *Sl4CL3* promoter. Statistical significance was determined by Student's *t*-test (*, $P<0.05$; **, $P<0.01$).

MdMYB306-like and PpMYB108, respectively. Two NAC Solyc04g005610 and Solyc06g069710 were clustered with known flavonoid regulators MusaATAF2-like and ANAC078, respectively. Solyc06g068830 and Solyc04g012050 belonging to AP2 family were clustered in same branch with AtERF114. One WRKY gene Solyc05g015850 showed compact cluster with a flavonoid regulator PbWRKY75. The above results suggest that two SlMYBs, two SlNACs, two SlAP2s, and one SlWRKY may be important regulators affected by SlMYB32 in flavonol or flavanone biosynthesis.

4. Discussion

4.1. Knockout of *SlMYB32* increased phytonutrient level in tomato

Modern diets recommend to increase consumption of fruit for phytonutrient supplements. Daily intake of flavonols and flavanones has potential benefits to human health (Ulusoy and Sanlier 2020). It was shown that rutin could lower lipid level and reduce inflammation in cholesterol metabolism disorders (Deng *et al.* 2024). Rutin could also be effective in relieving diabetic kidney disease (Dong *et al.* 2023). K3Rut, an important kaempferol derivative, showed excellent anti-inflammatory and anti-pyretic effects (Ruan *et al.* 2024; Zheng *et al.* 2024). Naringenin derivatives, especially N7Glc, have been found to inhibit protein damage to prevent diabetes complications (Ali *et al.* 2024). As shown in Figs. 4-E and 5-B, numerous flavonols and flavanones including rutin, K3Rut and N7Glc, were enriched in *SlMYB32* knockout mutants, indicating CRISPR/Cas9 targeting repressors could improve phytonutrient accumulation in fruit which is beneficial for health.

Meanwhile, knockout of *SlMYB32* resulted in orange-colored fruit (Fig. 4-D), which may be the result of elevated content of flavonols since quercetin derivatives and kaempferol derivatives are orange- or yellow-colored compounds. Previously, overexpression of *AtMYB12* in tomato resulted in elevated flavonol content in fruit, which caused orange color of fruit (Zhang *et al.* 2015). Recently, our group also produced orange-colored fruit by overexpression of *MrMYB12* in tomato

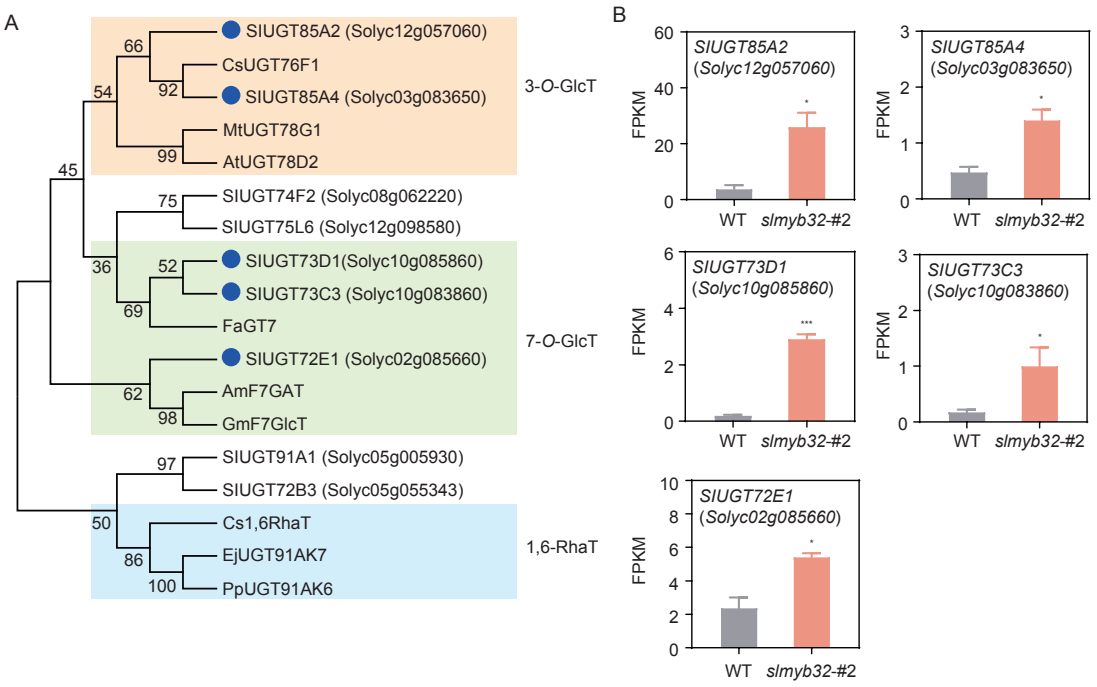


Fig. 8 Phylogenetic relationship and expression analysis of differentially expressed *SlUGT*s. A, phylogenetic analysis of candidate SlUGTs in *slmyb32* mutants. B, expression analysis of candidate *SlUGT*s in *slmyb32-#2* mutant. Statistical significance was determined by Student's *t*-test (*, $P<0.05$; ***, $P<0.001$). Accession number is listed as follows: *Arabidopsis thaliana* AtUGT78D2 (NP_197207); *Citrus sinensis* CsUGT76F1 (KDO69246), Cs1,6RhaT (NP_001275829); *Medicago truncatula* MtUGT78G1 (XP_003610163); *Fagaria×ananassa* FaGT7 (Q2V6J9); *Antirrhinum majus* AmF7GAT (BAG31945); *Glycine max* GmF7GlcT (NP_001235161); *Eriobotrya japonica* EjUGT91AK7 (Ej00065981); *Prunus persica* PpUGT91AK6 (XP_007217954).

with flavonol content of about 2 mg g^{-1} FW (Cao *et al.* 2024b). In the present study, about 1 mg g^{-1} FW Q3Rut as well as 0.1 mg g^{-1} FW K3Rut were detected in *slmyb32* mutants and we thought the color change might relate with the elevated contents of flavonoids. However, it is worthy to measure carotenoid content in the future and check whether SlMYB32 could regulate carotenoid biosynthesis in tomato.

4.2. Repressor SlMYB32 regulated early metabolic pathway and *SlUGT*s expression

R2R3-MYB TFs act as master regulators involved in flavonoid biosynthesis (Liu *et al.* 2015). There are increasing studies focused on R2R3-MYB repressors, which can be classified into two categories: AtMYB4-type repressors mainly regulating the phenylpropanoid pathway and FaMYB1-type repressors mainly regulating downstream structural genes involved in flavonoid biosynthesis (Ma and Constabel 2019). It was found that expression of *AtC4H* was increased in *atmyb4* mutant, and overexpression of *AtMYB4* down-regulated expression of *AtC4H*, *At4CL* and *At4CL3* (Jin *et al.* 2000). Down-regulation of *PvPAL*, *PvC4H*, and *Pv4CL* was detected in transgenic *Panicum virgatum* overexpressing *PvMYB4* (Shen *et al.* 2012). SlMYB32 had clustering relationship with AtMYB4 (Fig. 2-A), suggesting it might be a AtMYB4-type repressor. Similarly, SlMYB32 could bind to and repress promoter activities of *SlPAL6* and *Sl4CL3* to repress their expression (Fig. 7). However, SlMYB32 did not inhibit the promoter activity of *Sl4CL4*. The higher expression of *Sl4CL4* in *slmyb32* mutants might be caused by other transcriptional activator that was released with the absence of repressor SlMYB32 (Fig. 7-A), which can be verified in the future.

It was interesting that five *SlUGT*s, which were downstream biosynthetic genes in flavonoid pathway, were up-regulated in *slmyb32* mutants (Fig. 8). Phylogenetic analysis indicated that SlUGT85A2 and SlUGT85A4 were clustered with known 3-*O*-GlcTs, including CsUGT76F1 (Liu *et al.* 2018), MtUGT78G1 (Modolo *et al.* 2009) and AtUGT78D2 (Tohge *et al.* 2015). SlUGT73D1 and SlUGT73C3 possessed close clustering relation with FaGT7 (Griesser *et al.* 2008), which was reported as a 7-*O*-GlcT. SlUGT72E1 was clustered with two known 7-*O*-GlcTs, including AmF7GAT (Noguchi *et al.* 2009) and GmF7GlcT (Funaki *et al.* 2015). Therefore, SlUGT85A1, SlUGT85A4, SlUGT73D1, SlUGT73C3 and SlUGT72E1 might be important candidates involved in glucosylflavonoid biosynthesis, which may correspond to increased accumulation of flavonol and flavanone glycosides in *slmyb32* mutant (Figs. 4-E and 5-B).The above results indicate that AtMYB4-type repressor SlMYB32 is involved in flavonol and flavanone biosynthesis by regulating both the early phenylpropanoid pathway and UGT activity.

4.3. Different transcription factors might be involved in flavonol or flavanone biosynthesis

MYB TFs are known to regulate expression of numerous TFs involved in flavonoid biosynthesis. Mutagenesis of repressor *MtMYB2* resulted in up-regulation of *MtMYB5*, *MtMYB530*

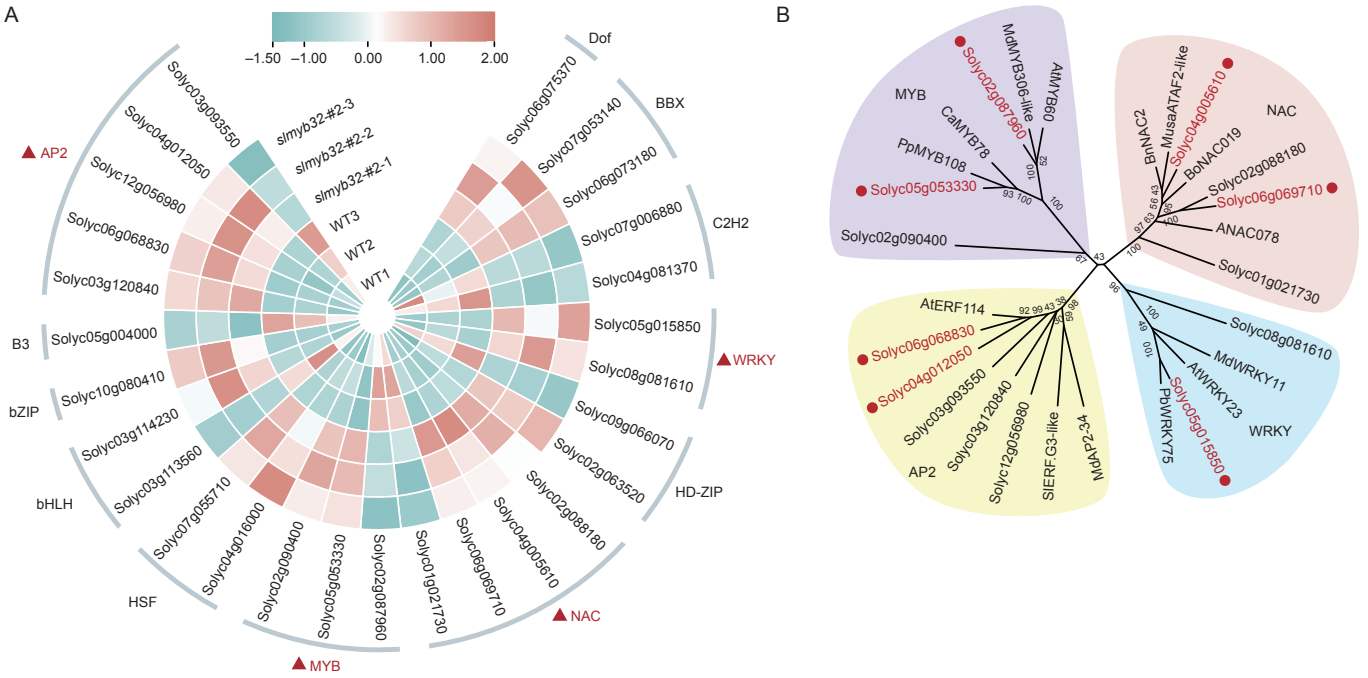


Fig. 9 Transcription factor analysis involved in flavonol and flavanone biosynthesis. A, expression heatmap of differentially expressed genes that encoded transcriptional factors. The expression profile was determined based on $\log_2$-transformed normalized FPKM in the RNA-seq data for each gene. B, phylogenetic analysis of differentially expressed MYBs, NACs, AP2s and WRKYs in tomato and other species. Accession number is listed as follows: *Arabidopsis thaliana* AtMYB60 (AAC83617), ANAC078 (NP_196061), AtERF114 (NP_200995), AtWRKY23 (NP_182248); *Malus domestica* MdMYB306-like (XP_028953285), MdAP2-34 (RXH68807), MdWRKY11 (XP_008356462); *Prunus persica* PpMYB108 (ONI27931); *Solanum lycopersicum* SlERF.G3-like (AP028936); *Cicer arietenum* CaMYB78 (XP_004495882); *Musa nana* MusaATAF2-like (UDE22644); *Brassica oleracea* BoNAC019 (XP_013588383); *Gossypium hirsutum* GhWRKY41 (XP_040931065).

and *MtMYB730* in *Medicago truncatula*, and MtMYB5 was manifested to act as an anthocyanin activator (Jun *et al.* 2015). Polar hairy roots overexpressing repressor *Populus MYB182* reduced expression of *MYB115* and *bHLH131*, which acted as positive regulators in proanthocyanidin accumulation (Yoshida *et al.* 2015). Similarly, we found expression of 27 DETFs belonging to 12 families were significantly changed in *slmyb32* mutant, of which nineteen DETFs were up-regulated and eight DETFs were down-regulated (Fig. 9-A). As for up-regulated DETFs, they might be directly or indirectly inhibited by SlMYB32. As for down-regulated DETFs, they might be inhibited by some repressors, which were released with the absence of SlMYB32. Meanwhile, previous studies reported that some transcription repressors and their partners might possess similar expression pattern, such as PhMYB27 and PhAN11 (Albert *et al.* 2014), FhMYB27, FhTT8L and FhTTG1 (Li Y *et al.* 2020). Therefore, the down-regulated DETFs might also be co-factors of SlMYB32.

Further phylogenetic analysis was conducted to explore the correlation between DETFs and flavonoid accumulation, where six transcription activators, i.e., one SlMYB, two SlNACs, two SlAP2s and one SlWRKY, and one repressor, i.e., SlMYB were identified (Fig. 9-B). One up-regulated MYB gene *Solyc05g053330* was clustered with an activator PpMYB108 involved in anthocyanin biosynthesis (Khan *et al.* 2022). One NAC gene *Solyc04g005610* was up-regulated in *slmyb32* mutant and clustered with MusaATAF2-like, which could promote narigenin accumulation (Bhakta *et al.* 2022). Solyc06g069710 had strong clustering relations with ANAC078, which was reported to be an activator inducing expression of *AtCHS*, *AtCHI*, *AtF3H* and *AtF3´H* (Morishita *et al.* 2009). Two AP2 genes *Solyc06g068830* and *Solyc04g012050* were up-regulated in *slmyb32* mutant and clustered with AtERF114, which was reported to activate *AtPAL1* expression (Li Z *et al.* 2022). Solyc05g015850 showed strong correlation with an anthocyanin activator PbWRKY75 (Cong *et al.* 2021). Besides the up-regulated DETFs, *Solyc02g087960* was down-regulated in *slmyb32* mutant and showed strong clustering relationships with MdMYB306-like, which was reported as an anthocyanin repressor (Wang *et al.* 2022). These results indicated SlMYB32 might form a transcriptional regulation network with these DETFs to regulate flavonol or flavanone biosynthesis.

5. Conclusion

In this study, we characterized a negative regulator SlMYB32 involved in flavonol and flavanone biosynthesis, and CRISPR/Cas9-mediated mutagenesis of *SlMYB32* results in flavonol-rich tomato with 1 mg g^{-1} FW rutin (Fig. 10). *SlPAL6*, *Sl4CL3* and *Sl4CL4* as well as five candidate *SlUGT*s were significantly up-regulated in *slmyb32* mutants. SlMYB32 was found to bind to and repress *SlPAL6* and *Sl4CL3* promoters to

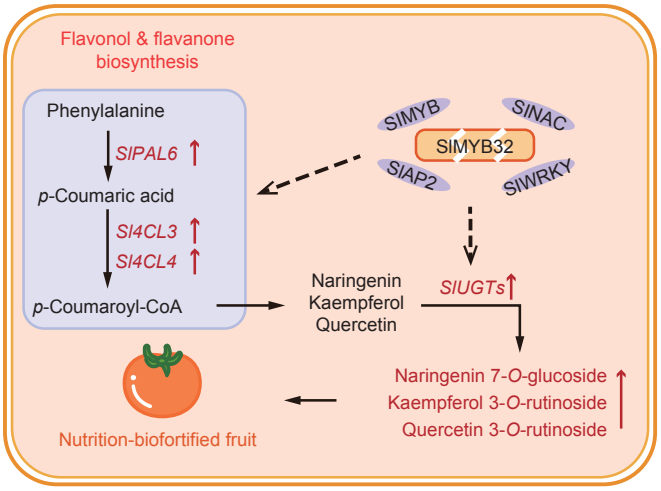


Fig. 10 A proposed model of SlMYB32-dominated flavonol and flavanone biosynthesis in biofortified tomato. CRISPR/Cas9-induced mutations in *SlMYB32* up-regulated expression of *SlPAL6*, *Sl4CL3*, *Sl4CL4* and *SlUGT*s. Meanwhile, several transcripton factors belonging to MYB, NAC, AP2 and WRKY families were regulated by SlMYB32 to involve in flavonol or flavanone biosynthesis. Directional mutation of *SlMYB32* resulted in flavonol- and flavanone-enriched tomato fruit.

regulate flavonol and flavanone biosynthesis. In addition, our study provided potential target TFs such as SlMYBs, SlNACs, SlAP2s and SlWRKYs, which can be further investigated for discovering transcriptional regulation network on flavonol or flavanone biosynthesis. This study suggests a promising approach for engineering nutrient-enriched fruit and provides new insights into the transcriptional repression of flavonol and flavanone biosynthesis.

Acknowledgements

The research was supported by the National Natural Science Foundation of China (32372667).

Declaration of competing interest

The authors declare that they have no conflict of interest.

Declaration of generative AI and AI-assisted technologies in the writing process

The authors declare that they did not use AI in the preparation and writing of this manuscript.

Data availability

The transcriptome sequencing data used in this study have been deposited in the NCBI database under accession number PRJNA1216022.

Appendices associated with this paper are available at https://doi.org/10.1016/j.jia.2025.11.011

References

Albert N W, Davies K M, Lewis D H, Zhang H, Montefiori M, Brendolise C, Boase M R, Ngo H, Jameson P E, Schwinn K E. 2014. A conserved network of transcriptional activators and repressors regulates anthocyanin pigmentation in eudicots. *The Plant Cell*, **26**, 962–980.

Ali M Y, Zamponi G W, Abdul Q A, Seong S H, Min B S, Jung H A, Choi J S. 2024. Prunin from *Poncirus trifoliata* (L.) Rafin inhibits aldose reductase and glucose-fructose-mediated protein glycation and oxidation of human serum albumin. *Journal of Agricultural and Food Chemistry*, **72**, 7203–7218.

Bhakta S, Negi S, Tak H, Singh S, Ganapathi T R. 2022. MusaATAF2-like protein regulates shoot development and multiplication by inducing cytokinin hypersensitivity and flavonoid accumulation in banana plants. *Plant Cell Reports*, **41**, 1197–1208.

Cao Y, Mei Y, Zhang R, Zhong Z, Yang X, Xu C, Chen K, Li X. 2024a. Transcriptional regulation of flavonol biosynthesis in plants. *Horticulture Research*, **11**, uhae043.

Cao Y, Zhang R, Ou R, Mei Y, Cui X, Zhang T, Yang X, Shi Y, Zhao X, Xu C, Chen K, Li X. 2024b. Overexpression of *MrMYB12* or *MrMYB12/MrF3'5'H* results in flavonol-rich tomato fruit that improves resistance against *Botrytis cinerea* during the shelf life period. *Postharvest Biology and Technology*, **211**, 112818.

Cao Y, Zhang R, Xing M, Ren C, Li J, Qian J, Mei Y, Yang X, Sun C, Grierson D, Chen K, Xu C, Li X. 2023. Synergistic actions of three MYB transcription factors underpins the high accumulation of myricetin in *Morella rubra*. *The Plant Journal*, **115**, 577–594.

Cavallini E, Matus J T, Finezzo L, Zenoni S, Loyola R, Guzzo F, Schlechter R, Ageorges A, Arce-Johnson P, Tornielli G B. 2015. The phenylpropanoid pathway is controlled at different branches by a set of R2R3-MYB C2 repressors in grapevine. *Plant Physiology*, **167**, 1448–1470.

Chen C, Wu Y, Li J, Wang X, Zeng Z, Xu J, Liu Y, Feng J, Chen H, He Y, Xia R. 2023. TBtools-II: A "one for all, all for one" bioinformatics platform for biological big-data mining. *Molecular Plant*, **16**, 1733–1742.

Cong L, Qu Y, Sha G, Zhang S, Ma Y, Chen M, Zhai R, Yang C, Xu L, Wang Z. 2021. PbWRKY75 promotes anthocyanin synthesis by activating *PbDFR*, *PbUFGT*, and *PbMYB10b* in pear. *Physiologia Plantarum*, **173**, 1841–1849.

Czemmel S, Stracke R, Weisshaar B, Cordon N, Harris N N, Walker A R, Robinson S P, Bogs J. 2009. The grapevine R2R3-MYB transcription factor VvMYBF1 regulates flavonol synthesis in developing grape berries. *Plant Physiology*, **151**, 1513–1530.

Deng X, Cheng L, Qiao Y, Liu X, Zhou Y, Liu H, Wang L. 2024. Rutin ameliorates HCD-induced cholesterol metabolism disorder in zebrafish larvae revealed by transcriptome and metabolome analysis. *Phytomedicine*, **135**, 156058.

Dong R, Zhang X, Liu Y, Zhao T, Sun Z, Liu P, Xiang Q, Xiong J, Du X, Yang X, Gui D, Xu Y. 2023. Rutin alleviates EndMT by restoring autophagy through inhibiting HDAC1 via PI3K/AKT/mTOR pathway in diabetic kidney disease. *Phytomedicine*, **112**, 154700.

Funaki A, Waki T, Noguchi A, Kawai Y, Yamashita S, Takahashi S, Nakayama T. 2015. Identification of a highly specific isoflavone 7-*O*-glucosyltransferase in the soybean (*Glycine max* (L.) Merr.). *Plant and Cell Physiology*, **56**, 1512–1520.

Gao Y, Lin Y, Xu M, Bian H, Zhang C, Wang J, Wang H, Xu Y, Niu Q, Zuo J, Fu D, Pan Y, Chen K, Klee H, Lang Z, Zhang B. 2022. The role and interaction between transcription factor NAC-NOR and DNA demethylase SlDML2 in the biosynthesis of tomato fruit flavor volatiles. *New Phytologist*, **235**, 1913–1926.

Griesser M, Vitzthum F, Fink B, Bellido M L, Raasch C, Munoz-Blanco J, Schwab W. 2008. Multi-substrate flavonol *O*-glucosyltransferases from strawberry (*Fragaria×ananassa*) achene and receptacle. *Journal of Experimental Botany*, **59**, 2611–2625.

Han X, Zhao S, Song H, Xu T, Fang Q, Hu G, Sun L. 2021. Kaempferol alleviates LD-mitochondrial damage by promoting autophagy: Implications in Parkinson's disease. *Redox Biology*, **41**, 101911.

Jin H, Cominelli E, Bailey P, Parr A, Mehrtens F, Jones J, Tonelli C, Weisshaar B, Martin C. 2000. Transcriptional repression by AtMYB4 controls production of UV-protecting sunscreens in *Arabidopsis*. *The EMBO Journal*, **19**, 6150–6161.

Jun J H, Liu C, Xiao X, Dixon R A. 2015. The transcriptional repressor MYB2 regulates both spatial and temporal patterns of proanthocyandin and anthocyanin pigmentation in *Medicago truncatula*. *The Plant Cell*, **27**, 2860–2879.

Khan I A, Cao K, Guo J, Li Y, Wang Q, Yang X, Wu J, Fang W, Wang L. 2022. Identification of key gene networks controlling anthocyanin

biosynthesis in peach flower. *Plant Science*, **316**, 111151.
Kumar S P, Birundha K, Kaveri K, Devi K T R. 2015. Antioxidant studies of chitosan nanoparticles containing naringenin and their cytotoxicity effects in lung cancer cells. *International Journal of Biological Macromolecules*, **78**, 87–95.
Li H, Li Y, Yu J, Wu T, Zhang J, Tian J, Yao Y. 2020. MdMYB8 is associated with flavonol biosynthesis via the activation of the *MdFLS* promoter in the fruits of *Malus* crabapple. *Horticulture Research*, **7**, 19.
Li J, Scarano A, Gonzalez N M, D'Orso F, Yue Y, Nemeth K, Saalbach G, Hill L, De Oliveira Martins C, Moran R, Santino A, Martin C. 2022. Biofortified tomatoes provide a new route to vitamin D sufficiency. *Nature Plants*, **8**, 611–616.
Li Y, Shan X, Gao R, Han T, Zhang J, Wang Y, Kimani S, Wang L, Gao X. 2020. MYB repressors and MBW activation complex collaborate to fine-tune flower coloration in *Freesia hybrida*. *Communications Biology*, **3**, 396.
Li Z, Zhang Y, Ren J, Jia F, Zeng H, Li G, Yang X. 2022. Ethylene-responsive factor ERF114 mediates fungal pathogen effector PevD1-induced disease resistance in *Arabidopsis thaliana*. *Molecular Plant Pathology*, **23**, 819–831.
Lin S, Li H, Tao Y, Liu J, Yuan W, Chen Y, Liu Y, Liu S. 2020. In vitro and in vivo evaluation of membrane-active flavone amphiphiles: Semisynthetic kaempferol-derived antimicrobials against drug-resistant gram-positive bacteria. *Journal of Medicinal Chemistry*, **63**, 5797–5815.
Liu G, Li C, Yu H, Tao P, Yuan L, Ye J, Chen W, Wang Y, Ge P, Zhang J, Zhou G, Zheng W, Ye Z, Zhang Y. 2020. *GREEN STRIPE*, encoding methylated TOMATO AGAMOUS-LIKE 1, regulates chloroplast development and Chl synthesis in fruit. *New Phytologist*, **228**, 302–317.
Liu J, Osbourn A, Ma P. 2015. MYB transcription factors as regulators of phenylpropanoid metabolism in plants. *Molecular Plant*, **8**, 689–708.
Liu X, Lin C, Ma X, Tan Y, Wang J, Zeng M. 2018. Functional characterization of a flavonoid glycosyltransferase in sweet orange (*Citrus sinensis*). *Frontiers in Plant Science*, **9**, 166.
Love M I, Huber W, Anders S. 2014. Moderated estimation of fold change and dispersion for RNA-seq data with DESeq2. *Genome Biology*, **15**, 550.
Ma D, Constabel C P. 2019. MYB repressors as regulators of phenylpropanoid metabolism in plants. *Trends in Plant Science*, **24**, 275–289.
Ma X, Zhang Q, Zhu Q, Liu W, Chen Y, Qiu R, Wang B, Yang Z, Li H, Lin Y, Xie Y, Shen R, Chen S, Wang Z, Chen Y, Guo J, Chen L, Zhao X, Dong Z, Liu Y G. 2015. A robust CRISPR/Cas9 system for convenient, high-efficiency multiplex genome editing in monocot and dicot plants. *Molecular Plant*, **8**, 1274–1284.
Modolo LV, Li L, Pan H, Blount J W, Dixon R A, Wang X. 2009. Crystal structures of glycosyltransferase UGT78G1 reveal the molecular basis for glycosylation and deglycosylation of (iso)flavonoids. *Journal of Molecular Biology*, **392**, 1292–1302.
Morishita T, Kojima Y, Maruta T, Nishizawa-Yokoi A, Yabuta Y, Shigeoka S. 2009. Arabidopsis NAC transcription factor, ANAC078, regulates flavonoid biosynthesis under high-light. *Plant and Cell Physiology*, **50**, 2210–2222.
Murata K, Kitano T, Yoshimoto R, Takata R, Ube N, Ueno K, Ueno M, Yabuta Y, Teraishi M, Holland C K, Jander G, Okumoto Y, Mori N, Ishihara A. 2020. Natural variation in the expression and catalytic activity of a naringenin 7-*O*-methyltransferase influences antifungal defenses in diverse rice cultivars. *The Plant Journal*, **101**, 1103–1117.
Noguchi A, Horikawa M, Fukui Y, Fukuchi-Mizutani M, Iuchi-Okada A, Ishiguro M, Kiso Y, Nakayama T, Ono E. 2009. Local differentiation of sugar donor specificity of flavonoid glycosyltransferase in Lamiales. *The Plant Cell*, **21**, 1556–1572.
Nonaka S, Arai C, Takayama M, Matsukura C, Ezura H. 2017. Efficient increase of □-aminobutyric acid (GABA) content in tomato fruits by targeted mutagenesis. *Scientific Reports*, **7**, 7057.
Pathak S, Regmi S, Nguyen T T, Gupta B, Gautam M, Yong C S, Kim J O, Son Y, Kim J-R, Park M H, Bae Y K, Park S Y, Jeong D, Yook S, Jeong J H. 2018. Polymeric microsphere-facilitated site-specific delivery of quercetin prevents senescence of pancreatic islets *in vivo* and improves transplantation outcomes in mouse model of diabetes. *Acta Biomaterialia*, **75**, 287–299.
Ren C, Guo Y, Xie L, Zhao Z, Xing M, Cao Y, Liu Y, Lin J, Grierson D, Zhang B, Xu C, Chen K, Li X. 2022. Identification of UDP-rhamnosyltransferases and UDP-galactosyltransferase involved in flavonol glycosylation in *Morella rubra*. *Horticulture Research*, **9**, uhac138.
Rodríguez-Leal D, Lemmon Z H, Man J, Bartlett M E, Lippman Z B. 2017. Engineering quantitative trait variation for crop improvement by genome editing. *Cell*, **171**, 470–480.e8.
Ruan Y, Zhu X, Shen J, Chen H, Zhou G. 2024. Mechanism of Nicotiflorin in San-Ye-Qing rhizome for anti-inflammatory effect in ulcerative colitis. *Phytomedicine*, **129**, 155564.
Saxena S, Pal L, Naik J, Singh Y, Verma P K, Chattopadhyay D, Pandey A. 2023. The R2R3-MYB-SG7 transcription factor CaMYB39 orchestrates surface phenylpropanoid metabolism and pathogen resistance in chickpea. *New Phytologist*, **238**, 798–816.
Shen H, He X, Poovaiah C R, Wuddineh W A, Ma J, Mann D G J, Wang H, Jackson L, Tang Y, Neal Stewart C, Chen F, Dixon R A. 2012. Functional characterization of the switchgrass (*Panicum virgatum*) R2R3-MYB transcription factor PvMYB4 for improvement of lignocellulosic feedstocks. *New Phytologist*, **193**, 121–136.
Shi Y, Dai Z, Chen K. 2024. Transcription factors involved in tomato fruit quality improvement. *Food Quality and Safety*, **8**, fyad050.
Tang Y, Zhang L, Sun R, Luo B, Zhou Y, Zhang Y, Liang Y, Xiao B, Wang C. 2023. Pulmonary delivery of mucus-traversing PF127-modified silk fibroin nanoparticles loading with quercetin for lung cancer therapy. *Asian Journal of Pharmaceutical Sciences*, **18**, 100833.
Tohge T, Fernie A R. 2016. Specialized metabolites of the flavonol class mediate root phototropism and growth. *Molecular Plant*, **9**, 1554–1555.
Tohge T, Nishiyama Y, Hirai M Y, Yano M, Nakajima J, Awazuhara M, Inoue E, Takahashi H, Goodenowe D B, Kitayama M, Noji M, Yamazaki M, Saito K. 2005. Functional genomics by integrated analysis of metabolome and transcriptome of Arabidopsis plants over-expressing an MYB transcription factor. *The Plant Journal*, **42**, 218–235.
Ulusoy H G, Sanlier N. 2020. A minireview of quercetin: From its metabolism to possible mechanisms of its biological activities. *Critical Reviews in Food Science and Nutrition*, **60**, 3290–3303.
Wang S, Zhang Z, Li L, Wang H, Zhou H, Chen X, Feng S. 2022. Apple MdMYB306-like inhibits anthocyanin synthesis by directly interacting with MdMYB17 and MdbHLH33. *The Plant Journal*, **110**, 1021–1034.
Xing M, Cao Y, Grierson D, Sun C, Li X. 2021a. The chemistry, distribution, and metabolic modifications of fruit flavonols. *Fruit Research*, **1**, 1–11.
Xing M, Cao Y, Ren C, Liu Y, Li J, Grierson D, Martin C, Sun C, Chen K, Xu C, Li X. 2021b. Elucidation of myricetin biosynthesis in *Morella rubra* of the Myricaceae. *The Plant Journal*, **108**, 411–425.
Yoshida K, Ma D, Constabel C P. 2015. The MYB182 protein down-regulates proanthocyanidin and anthocyanin biosynthesis in poplar by repressing both structural and regulatory flavonoid genes. *Plant Physiology*, **167**, 693–710.
Zhang Q, Ge J, Liu X, Wang W, Liu X, Yin X. 2022. Consensus co-expression network analysis identifies AdZAT5 regulating pectin degradation in ripening kiwifruit. *Journal of Advanced Research*, **40**, 59–68.
Zhang S, Zhu H. 2024. Development and prospect of gene-edited fruits and vegetables. *Food Quality and Safety*, **8**, fyad045.
Zhang Y, De Stefano R, Robine M, Butelli E, Bulling K, Hill L, Rejzek M, Martin C, Schoonbeek H J. 2015. Different reactive oxygen species scavenging properties of flavonoids determine their abilities to extend the shelf life of tomato. *Plant Physiology*, **169**, 1568–1583.
Zheng W, Wang H, Wang X, Li X, Hu J, Zi X, Zhou Y, Pan D, Fu Y. 2024. Kaempferol 3-*O*-rutinoside, a flavone derived from *Tetrastigma hemsleyanum* Diels et Gilg, reduces body temperature through accelerating the elimination of IL-6 and TNF-α in a mouse fever model. *Molecules*, **29**, 1641.

Executive Editor-in-Chief Sanwen Huang
Managing Editor Lingyun Weng